Electron Crystallographic Analysis of Two-Dimensional Streptavidin Crystals Coordinated to Metal-Chelated Lipid Monolayers

Wolfgang Frey,* Jacob Brink,# William R. Schief, Jr.,* Wah Chiu,# and Viola Vogel*
*Department of Bioengineering, University of Washington, Seattle, Washington 98195, and #National Center for Macromolecular Imaging, Verna and Marrs McLean Department of Biochemistry, Baylor College of Medicine, Houston, Texas 77030 USA

ABSTRACT Coordination of individual histidine residues located on a protein surface to metal-chelated lipid monolayers is a potentially general method for crystallizing proteins in two dimensions. It was shown recently by Brewster angle microscopy (BAM) that the model protein streptavidin binds via its surface histidines to Cu-DOIDA lipid monolayers, and aggregates into regularly shaped domains that have the appearance of crystals. We have used electron microscopy to confirm that the domains are indeed crystalline with lattice parameters similar to those of the same protein crystallized beneath biotinylated lipid monolayers. Although BAM demonstrates that the two-dimensional protein crystals grown via metal chelation are distinct from the biotin-bound crystals in both microscopic shape and thermodynamic behavior, the two crystal types show similar density projections and the same plane group symmetry.

INTRODUCTION

Two-dimensional (2D) protein crystallization beneath lipid monolayers (Uzgiris and Kornberg, 1983; Kornberg and Darst, 1991) has potential applications for the fabrication of nano-scale templates and is important in advancing high-resolution protein electron crystallography, because the projected structure of 2D crystals obtained by this technique is preserved in vitreous ice or glucose to 3-Å resolution (Kubalek et al., 1991; Avila-Sakar and Chiu, 1996). Moreover, 2D crystals of this type transferred to solid substrates have been used successfully as templates to initiate three-dimensional crystallization (Hemming et al., 1995). High-resolution structures have been obtained so far only from 2D crystals that have been formed via protein binding to high-affinity ligands (Chiu et al., 1997). However, the use of copper-chelated lipid monolayers to bind proteins via surface-accessible histidines (Shnek et al., 1994) can broaden the range of proteins that can be bound, oriented, and crystallized in two dimensions (Frey et al., 1996a). Quantitative optical techniques have been developed to probe protein adsorption and aggregation at interfaces under in situ conditions, including Brewster angle microscopy (BAM) (Frey et al., 1996b).

Here we present structural data demonstrating that streptavidin does indeed form 2D protein crystals when coordinated via its surface histidines to a copper-chelated lipid monolayer. In addition, we compare both the 2D-crystal projection structure and the thermodynamics of the crystallization process for streptavidin bound to copper-chelated lipid monolayers as well as to biotinylated lipid monolayers. Streptavidin is an ideal model system for investigating the influence of the surface binding mechanism on 2D protein crystallization, because its three-dimensional structure has been well characterized (Weber et al., 1989, 1992; Hendrickson et al., 1989; Pähler et al., 1987), and the 2D crystal structure of streptavidin bound to biotinylated lipid monolayers has been determined previously by electron crystallography (Kubalek et al., 1991; Avila-Sakar and Chiu, 1996). It is of considerable interest that the histidine residue responsible for coordination to the copper-chelated lipid monolayer, His^{87}, is located next to the entrance of the biotin binding pocket (Frey et al., 1996a). Thus the orientation of streptavidin with respect to the lipid monolayer is expected to be similar for both surface binding mechanisms. This close proximity of the two surface binding sites provides the opportunity to compare directly their crystallization behavior (Vogel et al., 1997) and 2D crystal structures.

MATERIALS AND METHODS

Two-dimensional crystal growth and quantitative BAM

To allow structural comparison with published 2D and 3D data, commercial streptavidin (Boehringer Mannheim) was used to grow 2D crystals in a home-built Langmuir trough of ~50-ml volume at room temperature as described earlier (Frey et al., 1996a,b). Monolayers of biotin-lipid (dipalmitoylphosphatidylethanolamine-X-biotin, DPPE-X-biotin; Molecular Probes) and metal-chelator-lipid (1,2-dioleyl-rac-glycero-3-(8–3,6-dioxy)octyl-1-amino-*N,N*-diacetic acid, Cu-DOIDA; premetallated DOIDA was generously provided by F. H. Arnold) (Fig. 1) were spread on a subphase containing 10 mM HEPES or 20 mM MOPS, respectively, as well as 250 mM NaCl, at pH 7.8. The lipid monolayer was then compressed to a surface pressure of 27 mN/m in the biotin-lipid case and ~3 mN/m in the Cu-DOIDA case. Protein was injected through the lipid monolayer to achieve a final protein concentration of ~2–6 μg/ml, and given at least 3 h to bind to the lipid and form crystals. The same lot of protein was used in the BAM experiments with both lipid types. Experiments with the chelator lipid were performed under argon atmosphere.

Received for publication 3 September 1997 and in final form 29 January 1998.

Address reprint requests to Dr. Viola Vogel, Department of Bioengineering, Box 357962, University of Washington, Seattle, WA 98195. Tel.: 206-543-1776; Fax: 206-685-4434; E-mail: vogel@bioeng.washington.edu.

Dr. Frey's present address is Department of Biomedical Engineering, Duke University, Box 90281, Durham, NC 27708-0281.

0006-3495/98/05/2674/06 $2.00

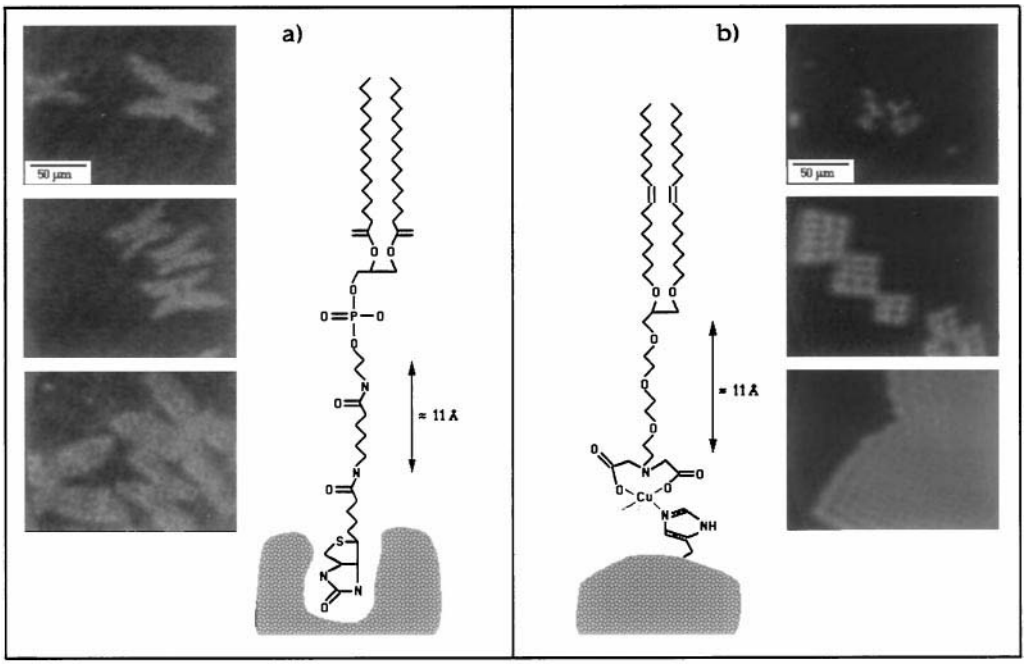

FIGURE 1 Two different mechanisms to bind streptavidin to a lipid monolayer at the air-water interface. (*a*) High-affinity binding to the ligand biotin and (*b*) coordination of histidines located on the protein surface to a divalent Cu-ion. The binding mechanism influences the shape and size of the 2D protein crystals. Images shown from top to bottom are taken 110, 115, and 170 min (*a*) and 15, 90, and 190 min (*b*) after protein injection.

The process of protein adsorption and crystal growth was observed by quantitative BAM. By using a Fresnel layer model and Maxwell-Garnet approximation, the reflected intensities captured in the image are converted to protein surface densities relative to the 2D protein crystal density (Frey et al., 1996b). The crystal density for streptavidin bound to a biotin-lipid monolayer has been determined by ellipsometry and neutron and x-ray reflectometry (Lösche et al., 1993; Herron et al., 1992; Schmidt et al., 1992). Based on the results of the 2D crystal structure analysis presented here, the relative protein density for the metal-chelator-lipid could also be estimated. For the calculation of the relative protein density, the optical parameters for the lipid layer were assumed to be the same as for the biotin-lipid (refractive index $n = 1.5$, monolayer thickness $d = 17$ Å). The error introduced by this assumption in calculating the protein density was estimated by varying both n and d over physically reasonable values (Maloney et al., manuscript submitted for publication). The protein surface density at which the first crystals occur is defined here as the critical surface density. Because this surface density is independent of protein bulk concentration (Frey et al., 1996b), the protein layer undergoes a 2D phase transition from fluid to crystalline.

Crystal transfer and transmission electron microscopy

Monolayers of Cu-DOIDA with bound streptavidin crystals were transferred to 400-mesh copper grids covered with a holey carbon film (Fukami and Adachi, 1965). The grids were rinsed in chloroform immediately before they were placed on the surface of the trough. The grids were lifted off the subphase with anticapillary tweezers, subsequently placed on a drop of water for 60 s, and finally stained with a 2% (w/v) aqueous solution of uranyl acetate (Ted Pella, Inc.) for 60 s.

Specimens of the 2D crystals were examined in a JEOL1200EX electron microscope operated at 100 kV. The samples were scanned for 2D crystals in defocused diffraction mode. Suitable areas were imaged at a precalibrated electron optical magnification of 37,364×, using low-dose techniques on Kodak SO-163 film, which was developed in full strength D-19 for 12 min at 20°C. Crystal images were inspected for crystallinity, lack of drift, and proper focus setting of the electron microscope's objective lens, by using an optical diffractometer. Suitable areas were digitized with a Perkin-Elmer 1010M microdensitometer at 3.5 Å/pixel or a Zeiss Phodis SCAI microdensitometer at 1.9 Å/pixel. Images were processed on a Silicon Graphics R10000 workstation, using the set of processing tools available in *I.C.E.* (Hardt et al., 1996). This included indexing the images' computed diffraction patterns, refining the reciprocal lattice vectors, straightening the crystal lattice in-plane bending, determining the contrast transfer functions of the images, evaluating the presence of crystalline symmetry, and merging multiple images by the cross-correlation method (Crowther et al., 1996; Henderson et al., 1986; Schmid et al., 1993; Thomas and Schmid, 1995). The combined structure factors from 7000 unit cells from four images were merged to compute the crystallographically averaged projected structure.

RESULTS AND DISCUSSION

Recently BAM has been applied to determine quantitatively the streptavidin surface density beneath lipid monolayers from a grayscale analysis of the images (Frey et al., 1996b). BAM further allows optimization of the 2D crystal growth conditions, because the visualization of the shape and size of the 2D crystals grown at the air/water interface enables one to select only high-quality monolayers for transfer onto transmission electron microscope (TEM) grids. Fig. 1 shows the structure of the two lipids used to bind streptavidin to the interface, together with a time sequence of representative BAM images for each lipid. Whereas affinity binding to the biotin-lipid induces elongated H-shaped domains that have been shown to be crystalline (Blankenburg et al., 1989; Darst et al., 1991), binding to the chelator-lipid Cu-DOIDA induces square domains. This difference in shape of the domains raised the question of whether the

Cu-DOIDA-bound streptavidin domains were crystalline, and whether the differences were related to genuine differences in the crystal structure or to kinetic effects.

Images obtained from negatively stained specimens of Cu-DOIDA-bound streptavidin, which revealed large aggregates by BAM, showed clear crystalline packing by electron microscopy (Fig. 2). The lattice parameters were determined as $a = 85.2$ Å, $b = 85.7$ Å (Table 1). For comparison, those for the biotin-bound 2D streptavidin crystals in vitreous ice were measured as $a = b = 82.3$ Å (Avila-Sakar and Chiu, 1996), and in negative stain as $a = b = 84$ Å (Darst et al., 1991). An analysis of the symmetry present in the 2D crystals of streptavidin complexed to the Cu-DOIDA lipids revealed that the phase residuals for the twofold symmetry along the lattice vectors are very similar to those for the vitreous ice-embedded crystals of streptavidin bound to biotin lipid (Table 1). This suggests that the plane group symmetry of the two crystals was the same, i.e., c222. The lower residuals for the stained crystals simply reflect the larger diffractive power caused by the stain. The relatively minor difference in the two lattice spacings is considered to reflect differences in preparative conditions. The reconstructed projection map of the Cu-DOIDA-bound streptavidin after merging data from several crystals is shown in Fig. 3. It resembles the view of the crystalline biotin-bound streptavidin viewed along the *R* dyad axis (cf. figure 7 in Avila-Sakar and Chiu, 1996). In this crystal form, there are two streptavidin tetramers per unit cell. Each tetramer has two monomeric subunits facing the lipid monolayer and the other two monomeric subunits facing away from the lipid monolayer. This mode of two-dimensional protein crystal packing would mean that half of each tetramer would be ligand-bound, and the other half would be ligand-free.

TABLE 1 Lattice vectors and phase residuals for twofold symmetry along the principal lattice vectors for streptavidin 2D crystals obtained using Cu-DOIDA lipids and DPPE-X-biotin lipids

	Lattice vectors (Å)		Phase residual (°)	
Crystal form	a^*	b^*	Along a^*	Along b^*
SA-Cu-DOIDA	85.2 (0.4)	85.7 (0.5)	5.9 (2.1)	12.4 (6.2)
SA-DPPE-X-biotin[#]	82.3	82.3	18.0	15.0
SA-DPPE-X-biotin[§]	84 ± 1	85 ± 1	5.3 [P2] 7.7 [C222]	

Numbers in parentheses denote the standard deviations over 58 measurements. The data for the DPPE-X-biotin lipids were obtained from ice-embedded crystals (Avila-Sakar and Chiu, 1996). For comparison, the results for DPPE-X-biotin bound streptavidin crystals, taken from Darst et al. (1991), are shown.
[#]Taken from Avila-Sakar and Chiu (1996).
[§]Taken from Darst et al. (1991).

The structural similarity between the two types of streptavidin crystals at 15-Å resolution contrasts not only with the differences in the macroscopic shape of the two crystals, but also with the different thermodynamic behaviors of the two systems as observed with BAM (Vogel et al., 1997). BAM is well suited to probing the adsorption process of streptavidin to the lipid monolayer, and to analyzing quantitatively the phase transition of monolayer-bound streptavidin from noncrystalline to crystalline. Fig. 4 shows the adsorption process and the noncrystalline to crystalline phase transition

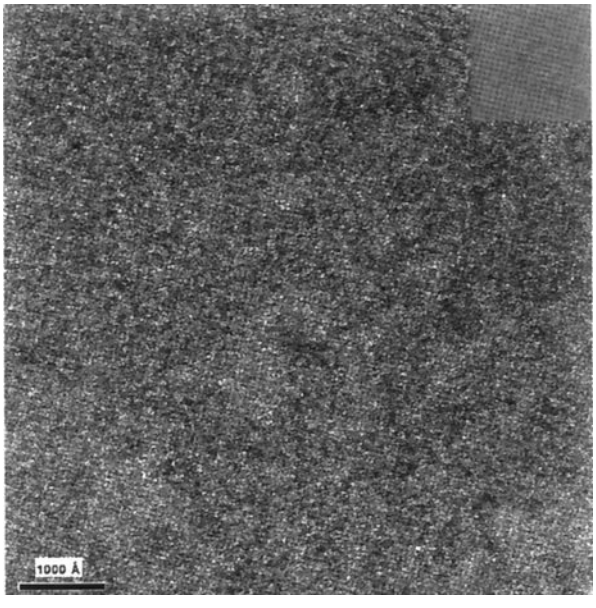

FIGURE 2 Digitized transmission electron microscopic image of a 2D streptavidin crystal grown beneath a Cu-DOIDA lipid monolayer. The crystal was negatively stained with uranyl acetate. The crystal area contains ~1700 unit cells. The bar is 1000 Å. The upper right part of the image has been Fourier filtered to enhance the visibility of the crystallinity features.

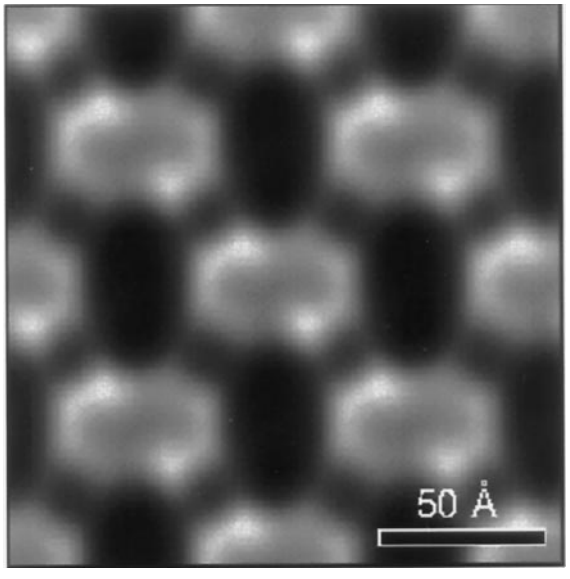

FIGURE 3 A 15-Å projected map of negative stained streptavidin 2D crystal formed beneath the Cu-DOIDA lipid monolayer. It was obtained after crystallographically merging image data from 7000 unit cells. The symmetry c222, which was applicable to biotin-bound streptavidin, was not enforced in this reconstruction. A single unit cell consisting of two tetramers is shown viewed along the *R* dyad axis. Protein is white.

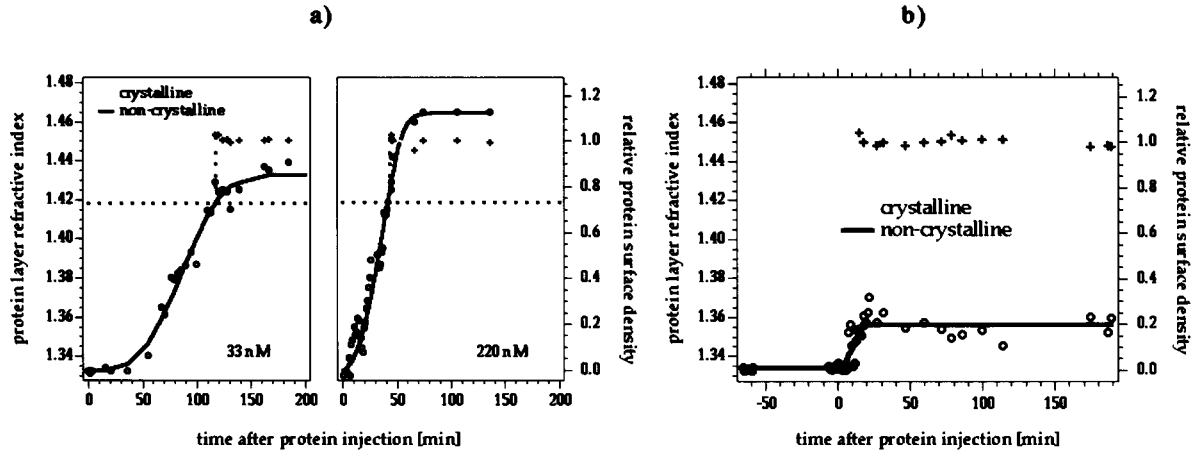

FIGURE 4 Refractive index of the protein layer and relative protein surface density, as deduced from grayscale analysis of BAM images taken while streptavidin binds from solution to (*a*) a biotin-lipid monolayer, and (*b*) a Cu-DOIDA monolayer. A constant critical surface density has to be reached to induce 2D crystallization. The relative protein surface density of the noncrystalline phase is constant in the phase coexistence region beneath Cu-DOIDA, but it rises in the case of the biotin-lipid. The time $t = 0$ marks the time of injection.

for both binding mechanisms, as extracted from BAM images after grayscale analysis.

Streptavidin bound to a biotin lipid needs ~60–120 min after injection, at bulk concentrations used here, before the first crystals appear at a critical protein surface density for the noncrystalline phase of 75% relative to the crystalline surface density. That the density of the noncrystalline phase increases after crystals appear is inconsistent with a first-order phase transition for a single-component system, in which a noncrystalline phase of constant density coexists with a crystalline phase (Fig. 4 *a*). Further investigation (Vogel et al., 1997) has revealed that the protein used in the experiments consists of two populations of truncated streptavidin, comprising residues 13–135 and 14–136, respectively. From the electron crystallographic study of biotin-bound 2D crystals of streptavidin, it can be concluded that the N- and C-terminal residues are located in the protein-protein contacts in the 2D crystal (Avila-Sakar and Chiu, 1996). Their absence or presence can potentially influence the crystallization behavior. Furthermore, it has been reported that the binding to biotin induces an asymmetry in the growth kinetics, with the longer and faster growing axis along a line parallel to the surface, which is directed through the two unoccupied biotin binding sites (Ku et al., 1993).

In contrast, streptavidin bound to Cu-DOIDA needs ~15 min after injection, for the bulk concentration used, before the first crystals appear at a relative protein surface density of 20 ± 10% of the crystalline surface density. It is remarkable that the density of this noncrystalline phase is constant, indicating a phase transition as expected for a single-component system, despite the fact that the same binary mixture of truncated streptavidins is used in this experiment (Fig. 4 *b*). The commercial streptavidin used here therefore reveals a subtle difference, whereas experiments with pure recombinant streptavidin show a pure first-order phase transition of a single-component system (Schief, manuscript in preparation).

It is clear that electron microscopic imaging reveals local features on a molecular level, whereas BAM gives information on a larger scale. The question is whether these two sets of observations can be correlated to give detailed insight into the crystallization process. Two sets of interpretation of our observations could be possible. The first hypothesis is that the thermodynamic dissimilarities in crystal shape, induction time, and critical protein surface density between the two binding mechanisms are caused by small structural differences in the proteins upon binding to the lipid monolayer. It is reasonable to assume that the binding to Cu-DOIDA induces less structural change in streptavidin than binding to biotin-lipid. For instance, it has been reported that binding of biotin induces a rearrangement of the C_α atoms in the monomers with a root mean square deviation ranging from 0.7 to 2.0 Å (Weber et al., 1989). In 2D crystals, the binding of two biotins on one side of the tetrameric molecule could also induce an asymmetry by only changing the structure of two occupied subunits. This asymmetry might induce different protein-protein attachment energies along the two growth directions and hence different growth kinetics. The binding of biotin may also induce changes in the C- and N-termini that sensitively influence the thermodynamic behavior. In our data, the c222 symmetry of the unit cell as well as the similarity of the unit cells for both binding mechanisms suggest no structural basis for the observed thermodynamic behavior. However, we cannot rule out the possibility that the structural changes are too small to detect at the current level of resolution.

Alternatively, the thermodynamic differences may originate primarily from kinetic effects. Because protein surfaces are complex, a protein may attach to the surface of a crystal in more than one way along each crystal growth direction (Garrone and Ugliengo, 1991; Noever, 1995; Frey et al.,

1991). Some of these attachments will not promote crystal growth, and therefore a protein will have to detach from the crystal surface to allow further growth. Because only those modes of attachment that promote crystal growth are represented significantly in the final equilibrium crystal, the crystal structure would not be affected by a change in number or relative probability of those attachment modes that do not support crystal growth. However, crystal size and shape as well as crystallization speed and nucleation kinetics would be strongly affected. Because the probability of finding a protein in one specific state of attachment is determined by the Boltzmann factor for that attachment energy, the growth rate increases with the energy difference between the growth-promoting and nonpromoting attachment states. Accordingly, a kinetic model to explain our observations postulates a large energy difference between the crystallization-promoting and the nonpromoting attachment states along the axis of the fast growing, biotin-free monomers, and a small difference along the slow growing axis of occupied monomers. The lack of a slow growing axis results in the square symmetrical shape of the Cu-DOIDA bound crystals. The height of the energy levels is likely to be sensitive to small changes in the composition of amino acid side chains close to or within the protein-protein contacts, thereby affecting the relative population of the two levels more severely if their energetic differences are small. This could explain the different sensitivities of biotin-bound and Cu-DOIDA-bound crystals to the presence of a heterogeneous mix of truncated streptavidins. It could also explain why no structural difference has been seen for biotin-bound streptavidin crystals along the fast and slow growing directions at 3.0-Å resolution (Avila-Sakar and Chiu, 1996). However, this asymmetry may exist, but may not have been observed because of the symmetrization of the data during the image analysis procedure used in that study. An alternative data-processing technique that averages small numbers of unit cells or single unit cell analysis that does not invoke Fourier averaging (Frank et al., 1988) may be able to determine if such an asymmetry is present.

In summary, we have shown that streptavidin does form 2D crystals via coordination of its surface histidines to Cu-DOIDA monolayers. The structural resolution of electron microscopy combined with in situ BAM grayscale analysis indicates that the pronounced differences in thermodynamic behavior resulting from the two binding methods are not based on structural differences large enough to be visible at the current resolution. Two models have been suggested. Whereas the influence of the N- and C-termini as well as the apparent miscibility gap associated with the phase transition in the biotin-bound case hint at small structural changes, the shape, the induction times, and the differences in the protein surface densities of the phase transition favor kinetic causes. Future experiments, combined with high-resolution diffraction data from DOIDA-bound streptavidin crystals, will be necessary to distinguish between the models proposed.

We gratefully acknowledge the collaboration with Frances Arnold and Dan Pack on protein binding to Cu-DOIDA lipid monolayers, as well as many discussions with Patrick Stayton on protein crystallization.

This work was supported through a National Institutes of Health training grant fellowship in Biotechnology, and subsequently in Molecular Biophysics, to WRS, and funding from NASA (NAG8-1149). JB and WC were supported by grants from the National Center for Research Resources of the National Institutes of Health (RR02250), the National Science Foundation (BIR9412521 and BIR9413229), and the Robert Welch Foundation.

REFERENCES

Avila-Sakar, A. J., and W. Chiu. 1996. Visualization of β-sheets and side-chain clusters in two-dimensional periodic arrays of streptavidin on phospholipid monolayers by electron crystallography. *Biophys. J.* 70: 57–68.

Blankenburg, R., P. Meller, H. Ringsdorf, and C. Salesse. 1989. Interaction between biotin lipids and streptavidin in monolayers: formation of oriented two-dimensional protein domains induced by surface recognition. *Biochemistry.* 28:8214–8221.

Chiu, W., A. J. Avila-Sakar, and M. F. Schmid. 1997. Electron crystallography of macromolecular periodic arrays on phospholipid monolayers. *Adv. Biophys.* 34:161–172.

Crowther, R. A., R. Henderson, and J. M. Smith. 1996. MRC image processing programs. *J. Struct. Biol.* 116:9–17.

Darst, S. A., M. Ahlers, P. H. Meller, E. W. Kubalek, R. Blankenburg, H. O. Ribi, H. Ringsdorf, and R. D. Kornberg. 1991. Two-dimensional crystals of streptavidin on biotinylated lipid layers and their interactions with biotinylated macromolecules. *Biophys. J.* 59:387–396.

Frank, J., W. Chiu, and L. Degn. 1988. The characterization of structural variations within a crystal field. *Ultramicroscopy.* 26:345–360.

Frey, M., J.-C. Genovesio-Taverne, and J. C. Fontecilla-Camps. 1991. Molecular packing and morphology of protein crystals. *J. Appl. Phys.* 24:105–110.

Frey, W., W. R. Schief, Jr., D. W. Pack, C.-T. Chen, A. Chilkoti, P. Stayton, V. Vogel, and F. H. Arnold. 1996a. 2-D protein crystallization via metal-ion coordination by naturally occurring surface histidines. *Proc. Natl. Acad. Sci. USA.* 93:4937–4941.

Frey, W., W. R. Schief, Jr., and V. Vogel. 1996b. Two-dimensional crystallization of streptavidin studied by quantitative Brewster angle microscopy. *Langmuir.* 12:1312–1320.

Fukami, A., and K. Adachi. 1965. A new method of preparation of a self-perforated micro plastic grid and its application (I). *J. Electron. Microsc. (Tokyo).* 14:112–118.

Garrone, E., and P. Ugliengo. 1991. Twofold adsorption of a molecule at the same site: the case of the isolated hydroxyl at the silica surface. *Langmuir.* 7:1409–1412.

Hardt, S., B. Wang, and M. F. Schmid. 1996. A brief description of I. C. E.: the integrated crystallographic environment. *J. Struct. Biol.* 116:68–70.

Hemming, S. A., A. Bochkarev, S. A. Darst, R. D. Kornberg, P. Ala, D. S. C. Yang, and A. M. Edwards. 1995. The mechanism of protein crystal growth from lipid layers. *J. Mol. Biol.* 246:308–316.

Henderson, R., J. M. Baldwin, K. H. Downing, J. Lepault, and F. Zemlin. 1986. Structure of purple membrane from *Halobacterium halobium*: recording, measurement and evaluation of electron micrographs at 3.5 Å resolution. *Ultramicroscopy.* 19:147–178.

Hendrickson, W. A., A. Pähler, J. L. Smith, Y. Satow, E. A. Merritt, and R. P. Phizackerly. 1989. Crystal structure of core streptavidin determined from multiwavelength anomalous diffraction of synchrotron radiation. *Proc. Natl. Acad. Sci. USA.* 86:2190–2194.

Herron, J. N., W. Mueller, M. Paudler, H. Riegler, H. Ringsdorf, and P. A. Suci. 1992. Specific recognition-induced self-assembly of a biotin lipid/streptavidin/Fab fragment triple layer at the air/water interface: ellipsometric and fluorescence microscopy investigations. *Langmuir.* 8:1413–1416.

Kornberg, R. D., and S. A. Darst. 1991. Two-dimensional crystals of proteins on lipid layers. *Curr. Opin. Struct. Biol.* 1:642–646.

Ku, A. C., S. A. Darst, C. R. Robertson, A. P. Gast, and R. D. Kornberg. 1993. Molecular analysis of two-dimensional protein crystallization. *J. Phys. Chem.* 97:3013–3016.

Kubalek, E. W., R. D. Kornberg, and S. A. Darst. 1991. Improved transfer of two-dimensional crystals from the air/water interface to specimen support grids for high-resolution analysis by electron microscopy. *Ultramicroscopy.* 35:295–304.

Lösche, M., M. Piepenstock, A. Diederich, T. Grünewald, K. Kjaer, and D. Vaknin. 1993. Influence of surface chemistry on the structural organization of monomolecular protein layers adsorbed to functionalized aqueous interfaces. *Biophys. J.* 65:2160–2177.

Noever, D. A. 1995. Kinetic effects in protein crystals. I. The role of hydration in protein aggregation. *J. Appl. Phys.* 28:1384–1392.

Pähler, A., W. A. Hendrickson, M. A. Gawinowicz Kolks, C. E. Argarana, and C. R. Cantor. 1987. Characterization and crystallization of core streptavidin. *J. Biol. Chem.* 262:13933–13937.

Schmid, M. F., R. Dargahi, and M. W. Tam. 1993. SPECTRA: a system for processing electron images of crystals. *Ultramicroscopy.* 48:251–264.

Schmidt, A., J. Spinke, T. Bayerl, E. Sackmann, and W. Knoll. 1992. Streptavidin binding to biotinylated lipid layers on solid supports. A neutron reflection and surface plasmon optical study. *Biophys. J.* 63: 1385–1392.

Shnek, D. R., D. W. Pack, D. Y. Sasaki, and F. H. Arnold. 1994. Specific protein attachment to artificial membranes via coordination to lipid-bound copper(II). *Langmuir.* 10:2382–2388.

Thomas, I. M., and M. F. Schmid. 1995. A cross-correlation method for merging electron crystallographic image data. *J. Microsc. Soc. Am.* 1:167–173.

Uzgiris, E. E., and R. D. Kornberg. 1983. Two-dimensional crystallization technique for imaging macromolecules, with application to antigen-antibody-complement complexes. *Nature.* 301:125–129.

Vogel, V., W. R. Schief, Jr., and W. Frey. 1997. Dynamics of 2-D protein crystallization at the air/water interface: streptavidin targeted to surfaces via high-affinity binding or metal coordination. *Supramol. Sci.* 4:163–171.

Weber, P. C., D. H. Ohlendorf, J. J. Wendoloski, and F. R. Salemme. 1989. Structural origins of high-affinity biotin binding to streptavidin. *Science.* 243:85–88.

Weber, P. C., J. J. Wendoloski, M. W. Pantoliano, and F. R. Salemme. 1992. Crystallographic and thermodynamic comparison of natural and synthetic ligands bound to streptavidin. *J. Am. Chem. Soc.* 114: 3197–3200.